

A suite-level review of the neutron powder diffraction instruments at Oak Ridge National Laboratory

Cite as: Rev. Sci. Instrum. **89**, 092701 (2018); <https://doi.org/10.1063/1.5033906>

Submitted: 06 April 2018 • Accepted: 19 July 2018 • Published Online: 28 September 2018

 S. Calder,  K. An, R. Boehler, et al.

COLLECTIONS

Paper published as part of the special topic on [Advances in Modern Neutron Diffraction](#)



View Online



Export Citation



CrossMark

ARTICLES YOU MAY BE INTERESTED IN

[A suite-level review of the neutron single-crystal diffraction instruments at Oak Ridge National Laboratory](#)




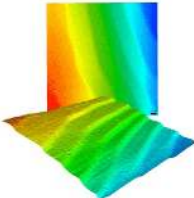

Review of Scientific Instruments **89**, 092802 (2018); <https://doi.org/10.1063/1.5030896>

[Preface: Special Topic on Advances in Modern Neutron Diffraction at Oak Ridge National Laboratory](#)

Review of Scientific Instruments **89**, 092601 (2018); <https://doi.org/10.1063/1.5055785>

[The high pressure gas capabilities at Oak Ridge National Laboratory's neutron facilities](#)

Review of Scientific Instruments **89**, 092907 (2018); <https://doi.org/10.1063/1.5032096>

	<p>Nanopositioning Systems</p> 	<p>Modular Motion Control</p> 	<p>AFM and NSOM Instruments</p> 	<p>Single Molecule Microscopes</p> 
---	--	--	---	--

A suite-level review of the neutron powder diffraction instruments at Oak Ridge National Laboratory

S. Calder,^{1,a)} K. An,¹ R. Boehler,^{1,2} C. R. Dela Cruz,¹ M. D. Frontzek,¹ M. Guthrie,^{3,4} B. Haberl,¹ A. Huq,¹ S. A. J. Kimber,¹ J. Liu,¹ J. J. Molaison,¹ J. Neufeind,¹ K. Page,¹ A. M. dos Santos,¹ K. M. Taddei,¹ C. Tulk,¹ and M. G. Tucker¹

¹Neutron Scattering Division, Oak Ridge National Laboratory, 1 Bethel Valley Rd., Oak Ridge, Tennessee 37831, USA

²Geophysical Laboratory, Carnegie Institution of Washington, Washington, District of Columbia 20015, USA

³European Spallation Source, Lund 221 00, Sweden

⁴University of Edinburgh, Edinburgh EH8 9YL, United Kingdom

(Received 6 April 2018; accepted 19 July 2018; published online 28 September 2018)

The suite of neutron powder diffractometers at Oak Ridge National Laboratory (ORNL) utilizes the distinct characteristics of the Spallation Neutron Source and High Flux Isotope Reactor to enable the measurements of powder samples over an unparalleled regime at a single laboratory. Full refinements over large Q ranges, total scattering methods, fast measurements under changing conditions, and a wide array of sample environments are available. This article provides a brief overview of each powder instrument at ORNL and details the complementarity across the suite. Future directions for the powder suite, including upgrades and new instruments, are also discussed. © 2018 Author(s). All article content, except where otherwise noted, is licensed under a Creative Commons Attribution (CC BY) license (<http://creativecommons.org/licenses/by/4.0/>). <https://doi.org/10.1063/1.5033906>

I. INTRODUCTION

Understanding the microscopic structure is often the first step in new materials discovery and is essential to improve the materials functional properties. Neutron powder diffraction has long been the technique of choice for structural characterization by solid-state chemists, material scientists, engineers, mineralogists, and condensed matter physicists for a large variety of materials ranging from strongly correlated-electron systems to energy-related materials to organic compounds. Neutron powder diffraction has played a primary role in crystal and magnetic structure determination and contrast resolution for elements that cannot be distinguished by x-rays. In addition, the study of materials under extreme conditions is particularly well suited to neutron diffraction since developing specialized sample environments can often be more straightforward than for x-ray diffraction due to the high penetration depth of neutrons in most materials. As the problems tackled by the structural tools get more and more complex, better instrumentation, faster data collection, higher Q-resolution, more complex sample environments, and modern modeling tools to extract the information are required.

The powder suite at Oak Ridge National Laboratory (ORNL) offers unique and complementary capabilities to tackle forefront scientific challenges. The ORNL neutron scattering facility consists of two co-located world class sources: the Spallation Neutron Source (SNS) and the High Flux Isotope Reactor (HFIR). The distinct neutron beam characteristics at SNS and HFIR offer unparalleled capabilities at

a single facility. The time-of-flight (TOF) scattering at the SNS excels at full refinements over large Q ranges and total scattering methods, while the high constant flux at the HFIR has unmatched performance for looking at a chosen limited range of Q and performing fast measurements of nuclear and magnetic peaks under changing conditions. ORNL currently hosts six neutron powder diffractometers, with future instruments planned to complement the suite. Current instruments at the SNS include: a high flux neutron powder diffraction/total scattering instrument Nanoscale Ordered Materials Diffractometer (NOMAD) for fast measurements and small samples, including liquids, glasses, and nanostructured materials; a third generation powder diffractometer POWGEN providing a single histogram data set over a wide Q range to access large unit cells, detailed structural refinements, and *in situ* chemical measurements; a dedicated high pressure beamline Spallation Neutrons and Pressure (SNAP) capable of measurements over a wide temperature and pressure range; and VULCAN which provides opportunities for materials and engineering systems testing and understanding under extreme stimuli. Current instruments at the HFIR include: a constant wavelength diffractometer HB-2A, with incident beam polarization option, capable of accessing exotic magnetic states with ultra-low temperature, magnetic field, and high-pressure sample environments and WAND², a dual-purpose powder and single-crystal diffractometer that offers a flexible sample environment and fast data acquisition. The powder suite instruments can be considered mature, although several recent upgrades have offered essentially new instrument capabilities. Sample environment options within the suite are impressive and continually developing. Advances are also on-going for data acquisition and analysis software, detectors, and detector coverage.

^{a)} Author to whom correspondence should be addressed: caldersa@ornl.gov

II. INSTRUMENT DESCRIPTIONS

A. NOMAD

The Nanoscale Ordered Materials Diffractometer (NOMAD) is a high-flux, low-to-medium-resolution diffractometer for structural characterization of both local order in liquids, solutions, glasses, polymers, nanocrystalline, and disordered bulk materials, as well as time-resolved and sample size limited structure determination in long-range ordered polycrystalline materials.

1. Instrument characteristics

A primary characteristic of NOMAD is high incident flux and large detector coverage leading to the highest neutron count rate for a given sample size (Table I).¹ This enables the study of small sample sizes and *in situ* observations of structural evolutions in an increasingly diverse array of environments, such as the aerodynamic levitator as shown in Fig. 1.

The layout of the instrument has NOMAD facing the decoupled poisoned supercritical hydrogen moderator at the SNS. The scattered beam is collected by a wide coverage of ³He detectors that are arranged in 6 banks, see Fig. 1. To achieve the highest solid angle coverage within a reasonable cost, many of the ³He tubes are in an unconventional horizontal arrangement, which is a unique design feature of this instrument. For a typical 2.54 cm diameter ³He position sensitive detector, the resolution along the tube is about 0.8 cm and if everything else is equal d- or Q- resolution is higher in this orientation since the high spatial resolution is perpendicular to the Debye Scherrer cone. At present, only 50% of the available detector positions are populated and this provides a clear upgrade path to increase the count rate, see Sec. IV A.

The NOMAD instrument sees dual use as a high flux TOF neutron diffractometer and a specialized total scattering beamline for neutron pair distribution function (PDF) studies. Typical powder diffraction studies, excluding those involving high d-spacings, utilize histogrammed data from the medium to high angle banks (those centered at 31°, 65°, 120.4°, and 150.1° 2 θ). Representative data are shown in Figs. 1(c)–1(f) for Si NIST standard material 640d, measured in a 6 mm diameter vanadium canister for 30 min at room temperature in the linear sample shifter at NOMAD.

As the average scattering angle is increased, the Q-range, maximum Q and minimum Q decrease, the resolution increases, and the peak shapes become more asymmetric. While the 31° and 65° NOMAD detector bank data are modeled well with standard TOF exponential peak profile parameters, the higher resolution bank data centered at

120.4° and 150.1° 2 θ are best fit with fundamental parameter approaches that take moderator line shape into effect.² Also, while it is typical to fit these four histograms, or a selection of these four histograms, for crystalline and nanocrystalline material diffraction studies on NOMAD, it is also possible to select unique detector groupings or any number/character of fit histograms to match the needs of specific experiments.

As a general observation, sample environments such as the orange cryostat, which allows for sample temperature to 1.5 K through flowed helium, and the ILL furnace, a mainstay for neutron diffraction for a long time built with vanadium heating elements and can achieve 1200 C, are not as well adapted to the small sample sizes and fast acquisition times at NOMAD, due to their relatively large background scattering and long equilibration times. A fast, low background, alternative is the Oxford Cobra cryostream system operated with argon gas that covers the temperature range from 90 to 500 K and has become a workhorse sample environment on NOMAD for samples in quartz capillaries and in vanadium canisters. A few of the unique sample environment capabilities offered at NOMAD, such as high temperature aerodynamic levitation [Fig. 1(a)] and gas flow capabilities, are reviewed in Sec. III. A cryofurnace system combined with a 20-position sample changer is currently being designed for NOMAD, to be delivered in 2019.

2. Science examples

The characteristics of NOMAD have enabled, for example, exemplary studies of alloys and melts via container-less levitation at extreme high temperatures with and without isotopic substitution,^{3,4} of the atomic structure of light atom species on nanomaterial surfaces and interfaces,^{5,6} of *in situ* material crystallization or growth,^{7–9} of materials synthesized through extreme conditions such as high pressure or swift ion irradiation,^{10,11} and of structure-property relationships in batteries,^{12,13} catalysts,^{14–16} thermoelectrics,¹⁷ and a host of other functional material families.

B. POWGEN

POWGEN is the highest resolution instrument in the powder suite and is optimized for both parametric studies of materials under a wide range of conditions and *ab initio* crystal structure determinations of complex solid-state materials with asymmetric unit-cells of the order $\sim 1500 \text{ \AA}^3$.

1. Instrument characteristics

POWGEN is a fundamental departure from previous designs for a TOF powder diffractometer at a spallation neutron source and may be considered a third-generation design.^{18,19} The geometric construct of the instrument allows

TABLE I. BL-1B NOMAD instrument specifications.

Applications	Neutron beam	Resolution ($\Delta d/d$)	Q-range	Beam size at sample	Measurement times
Total scattering (PDF); high flux measurements; high throughput capabilities. Small samples	TOF (decoupled poisoned supercritical hydrogen moderator)	5×10^{-3} to 5×10^{-2}	0.2-50 \AA^{-1} (see Fig. 1 for coverage of separate detector banks)	Variable. Typical is $0.6 \times 0.6 \text{ cm}$	Sample dependent, typical range is 1-60 min.

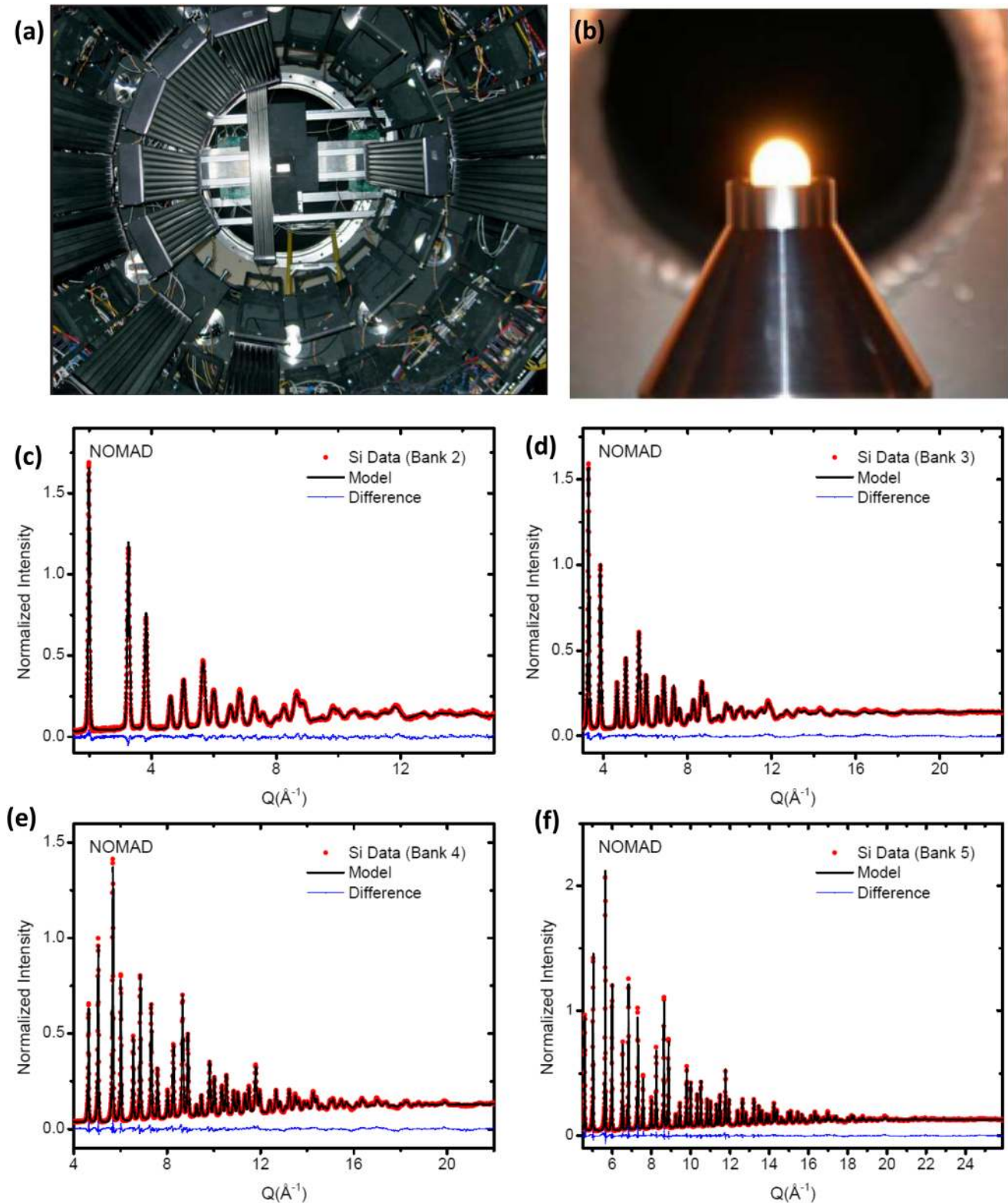


FIG. 1. (a) Inside of the NOMAD detector tank and (b) a sample (5 mm diameter) being measured on the aerodynamic levitator. [(c)-(f)] Si 640d data, shown with results of Rietveld refinement from the four highest angle standard detector groupings on NOMAD (detector banks centered at approximately 31° , 65° , 120° , and 150° 2θ). The Si was in a 6 mm diameter vanadium canister, and measurements were carried out for 30 min at room temperature in the linear sample shifter at NOMAD. Refinements were performed with Topas.

for all detected scattered neutrons to be focused onto a single diffraction profile yielding a high count rate with varying resolution as a function of d-spacing, preserving good resolution of $\Delta d/d = 0.0015$ at $d = 1 \text{ \AA}$ (Table II).

POWGEN was recently rebuilt to increase detector coverage and extend the coverage in Q , while still maintaining the original 3rd generation design philosophy. The detector coverage after the upgrade is 1.2 sr ($\sim 12 \text{ m}^2$ coverage).

TABLE II. BL-11A POWGEN instrument specifications.

Applications	Neutron beam	Resolution ($\Delta d/d$)	Q-range	Beam size at sample	Measurement times
General purpose powder diffraction; high throughput sample capabilities	TOF (decoupled poisoned super critical H ₂)	1×10^{-3} - 2.5×10^{-2}	0.7-50 \AA^{-1} (one frame). 0.15-50 \AA^{-1} (multiple frames)	40 \times 10 mm	Typically minutes to hours (depends on sample quantity, crystallinity, and symmetry)

A picture of the upgraded instrument is shown in Figs. 2(a) and 2(b).

During an experiment there is flexibility to vary the incident wavelengths over a wide range through control of adjustable bandwidth-limiting choppers and pulse repetition rates. With the current instrument configuration, any wavelength between 0.1 and 5 \AA at 60 Hz can be chosen with reasonable flux on samples [$\sim 10^7$ n/(\AA /MW-s)- 5×10^6 n/(\AA /MW-s)]. Typically, the instrument team selects and calibrates a fixed number of the center wavelength bands that cover differing ranges of d-spacings, as shown in Table III. Measurements outside of these settings are possible but require additional time to allow for collection of vanadium, a standard sample for profile calibration and empty background runs for proper normalization of data. The bandwidth choppers also allow operation in pulse skipping mode at 10, 20, and 30 Hz which increases the bandwidth accordingly but decreases flux. Interchangeable guide sections and the ability to trade resolution for intensity at the analysis stage allow users great latitude to optimize the data range, resolution, and statistical precision for each experiment. To reduce the background, the T zero chopper eliminates most of the prompt pulse and the software removes the small fraction of the prompt pulse (~ 50 μ s) before time focusing the data.

The instrument can cover d-spacings from ~ 0.1 \AA to 8 \AA in a single measurement at WL center 0.8 \AA ideal for both traditional Rietveld data and PDF measurements, albeit for significantly longer collection time than dedicated PDF machines, such as NOMAD. Rietveld measurements for traditional neutron-size samples (2-3 cc) can be completed in an hour or less, with a $<0.1\%$ resolution at short d-spacings and $<2.5\%$ resolution for nearly all d-spacings of interest. Alternatively, much of this resolution can be traded for increased intensity, making it possible to take shorter measurements while still maintaining good resolution using the high intensity guide. The high intensity guide gives a factor of 1.2, 1.8, and 2.2 gain at center wavelength 0.8, 1.5, and 2.665, respectively, at 60 Hz making it possible to collect data from smaller samples.

2. Science examples

Scientific studies on POWGEN encompass a wide range of novel materials. These include, but are not limited to, structural studies of energy storage materials such as battery materials,²⁰⁻²² ceramic membranes for solid oxide fuel cells and oxygen sensors, hydrogen storage materials,^{23,24} and thermoelectric materials.^{25,26} Fast data collection provides the ability to look at processes *in situ*, while the availability of long d-spacings also enables the study of magnetic materials such as high-T_c superconductors, metal-insulator phase transitions,

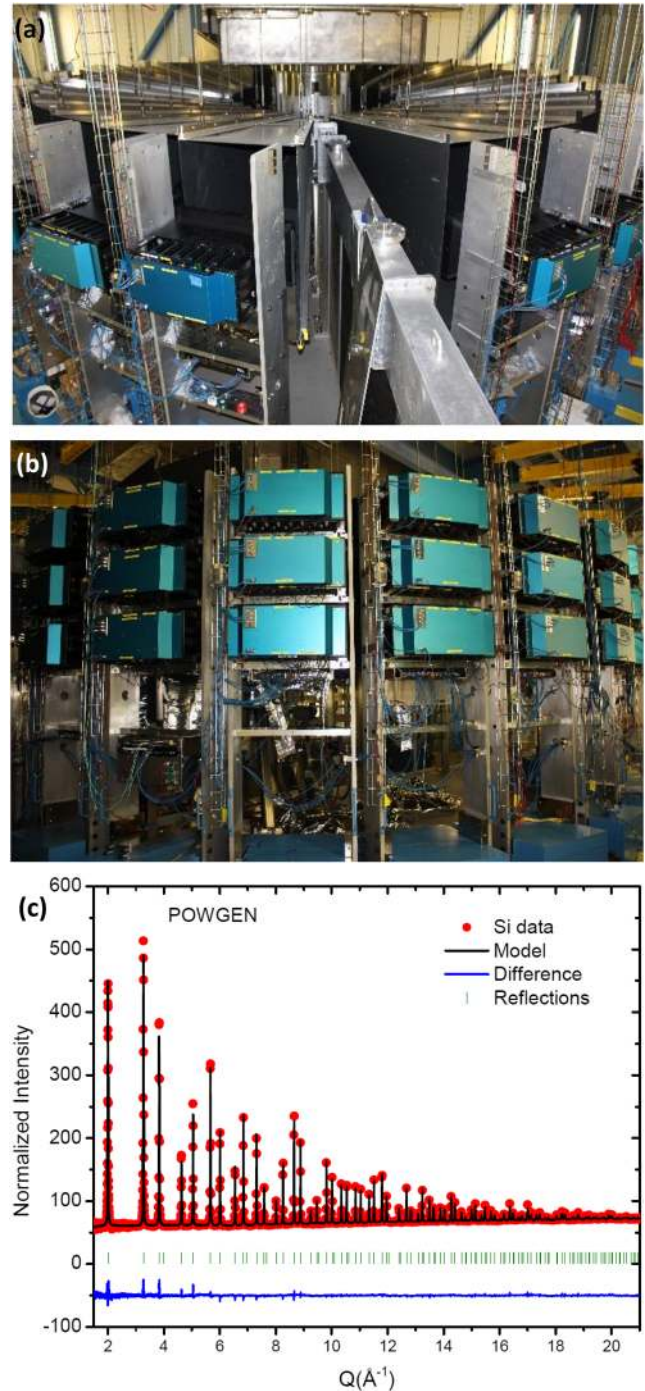


FIG. 2. Images of the POWGEN instrument after the recent upgrade and detector reconfiguration. (a) View along incident neutron guide. (b) Outside of the detector array, each module is 0.3 m² in size. (c) 1 g of the Si NIST standard SRM-640d sample was loaded in a V can. Data were collected for 11 C charge of the accelerator which corresponds to 3 beam hours using center wavelength 0.7 \AA . All 40 detectors were focused to 90°, and the data were reduced using the following formula Normalized I observed = (Sample - Empty 6 mm V can)/(V rod corrected for absorption and multiple scattering - V empty). Rietveld refinement was carried out using GSAS-II.

TABLE III. Standard wavelength (WL) settings on POWGEN showing the corresponding d and Q ranges.

Frequency	WL center	WL min	WL max	d_{\min} (Å)	d_{\max} (Å)	Q_{\min} (Å ⁻¹)	Q_{\max} (Å ⁻¹)
60	0.800	0.267	1.333	0.134	8.200	0.766	46.9
60	1.500	0.967	2.033	0.485	14.000	0.449	12.9
60	2.665	2.132	3.198	1.070	22.200	0.283	5.9
60	4.797	4.264	5.33	2.140	33.000	0.190	2.9
30	1.066	0.100	2.132	0.100	15.000	0.411	62.8
20	1.599	0.100	3.198	0.100	20.000	0.274	62.8
10	3.198	0.100	6.396	0.100	40.000	0.137	62.8

charge and orbital ordering transitions, and molecular magnets.^{27,28} POWGEN capabilities can contribute to understanding materials such as zeolite and Metal Organic Frameworks (MOF), metals and semiconductors; dielectrics, ferroelectrics; and *ab initio* structure solutions of complex polycrystalline materials such as pharmaceutical compounds.

C. SNAP

The Spallation Neutrons and Pressure (SNAP) instrument is a high-flux, medium-resolution diffractometer designed specifically to accommodate a variety of pressure cells for *in situ* studies of samples under the extreme conditions of high pressure and high/low temperature.

1. Instrument characteristics

The design philosophy of SNAP leveraged the enhanced neutron flux at SNS by building an instrument around an entire suite of standard and novel pressure cells (Table IV). This philosophy required an open walk-up sample location, rather than the conventional well design, that allows for easy sample alignment and pressure cell shielding to minimize background, see Fig. 3(a). For large sample volumes, the incident beam can be shaped by a straight evacuated flight tube for reduced background and highest available resolution. Alternatively, for smaller samples, a parabolic mirror guide can be used which increases the neutron flux by a factor of six across all wavelengths. The nominal beam size is 10×10 mm; however, in most cases a custom collimator is fitted as close as possible to the sample to minimize background and possible spurious Bragg scattering from components of the pressure device. Consequently, the typical illuminated area ranges from less than 1 mm^2 up to 3 mm^3 . One unique feature of this instrument is that, although most measurements are on powder samples, it is fitted with state-of-the-art Anger camera area detectors with sub-millimeter resolution suitable for single crystal measurements. The detector array consists of two square banks (0.45 m edge length) of 3×3 Anger camera modules, one on each side of the sample position.

Their 2θ location can be independently adjusted between 50° and 115° . This allows a Q -range of 0.5 \AA^{-1} – 25 \AA^{-1} at maximum coverage.

Due to the inherent versatility regarding incident optics, sample alignment, and detector array, the SNAP instrument excels at measurements in a variety of high pressure devices. These include conventional pressure devices such as the gas pressure and clamped cells, shared across the facility, and a dedicated suite of Paris-Edinburgh (PE) cells. These cells cover the typical pressure and temperature ranges already available at other facilities (see Table VIII). There are continued efforts at ORNL to improve the performance by incorporating radial collimators for gas/clamp pressure cells, as described elsewhere in the current issue. In addition, SNAP has been critical in the development of a new generation of diamond anvil cells (DACs) that enable a much wider pressure range, with smaller samples and are more amenable to heating and cooling.^{29,30} The new DACs benefit from advances in chemical vapor deposition methods for the growth of large single crystal diamonds and an entirely new cell and gasket design.²⁹ These allow for collection of refinable data above 60 GPa,³¹ but a custom design resulted in unprecedented measurements at close to 100 GPa.³² The new design is now standardized for use up to 40 GPa and down to 5 K, and is compatible with gas loading, a necessary condition to perform measurements in quasi-hydrostatic conditions. The use of these DACs for single crystal measurements has also been demonstrated and is detailed elsewhere in this issue of the journal.

2. Science examples

The science performed on SNAP is broad, reflecting the diverse research areas where the application of high pressure is relevant. For example, many important insights have been gained into areas of materials science ranging from magneto-structural correlations in magnetic dimers³⁵ or cubic perovskites³⁶ to insights into martensitic transitions in light elements³⁷ to the high-pressure synthesis of ultra-strong

TABLE IV. BL-3 SNAP instrument specifications.

Applications	Neutron beam	Resolution ($\Delta d/d$)	Detector coverage	Beam size at sample	Measurement times
High pressure studies	TOF (decoupled poisoned supercritical hydrogen moderator)	8×10^{-3} (at $2\theta = 90^\circ$)	$\Omega = 1.39$ sr $Q = 0.8\text{-}30 \text{ \AA}^{-1}$	Typical, $1 \text{ cm}^2 < 1 \text{ mm}^2$ for DACs	1-8 h, depending on sample size and scattering properties

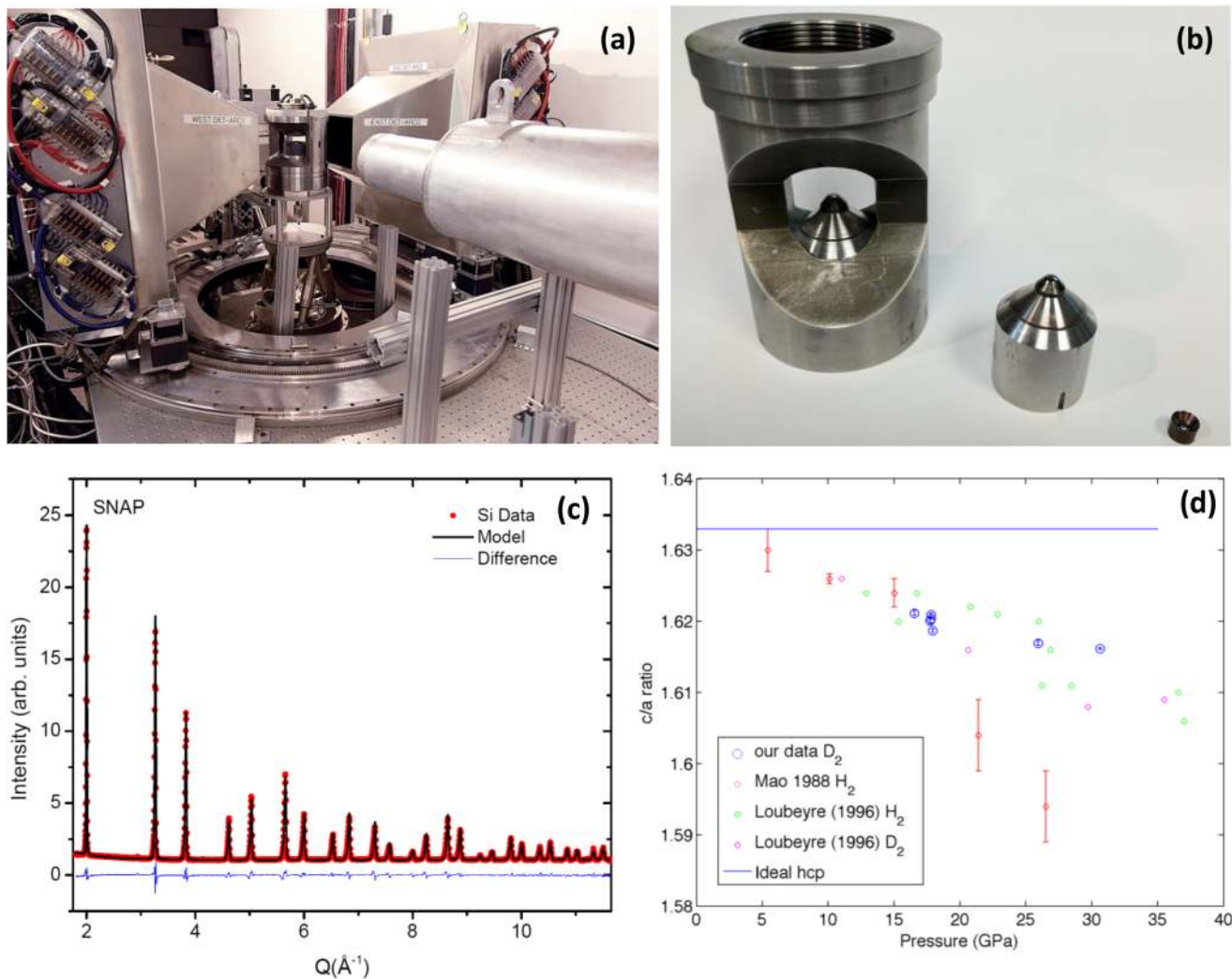


FIG. 3. (a) SNAP instrument sample area and detectors. The open layout allows for ease of access and a variety of pressure capabilities. A DAC measurement at room temperature is shown. (b) DAC shown on a bench-top, sample of area of order mm and cell height several inches. (c) Si data collected on SNAP. The Si was loaded into a vanadium can and measurements were carried out with the instrument flight tube (no guide), background-subtracted and normalized to vanadium. (d) The pressure-dependence of the c/a ratio of D_2 extracted up to 31 GPa at room temperature on SNAP in a diamond anvil cell compared to previous results in the literature.^{33,34}

diamond nanothreads.^{10,38} Additionally, the formation and behavior of various clathrates and hydrates have been investigated.^{39,40} Important contributions have also been made to the understanding of planetary ices such as water ice and further geophysical problems.^{31,41}

As a specific example, a unique system of study for the SNAP instrument is hydrogen (deuterium) and hydrogen-rich superconducting compounds such as H_2S , where the strong, coherent scattering cross section of deuterium allows neutron measurements to excel over x-ray techniques. D_2 was investigated on SNAP up to 31 GPa at room temperature, with the set-up yielding the first high pressure powder, rather than crystal, diffraction of this material. Rietveld refinement of the data allowed extraction of the c/a ratio which is well determined in a powder diffraction measurement, see Fig. 3(d). The resulting data show far less scatter than previous measurements which employed x-ray diffraction techniques using single-crystals. Our neutron c/a ratio is in broad agreement with the majority of past experiments, which all deviate from the ideal value

of 1.633 and show no strong evidence of isotope effects. An exception is Mao *et al.*'s 1988 x-ray study³³ of H_2 , which appears anomalous. The c/a ratio measured here with powder diffraction on snap appears to have a significantly lower dependence on pressure than the x-ray measurements. The reason for this is unclear motivating further studies to higher pressures.

D. VULCAN

VULCAN, the engineering materials diffractometer at SNS,⁴² is a versatile TOF instrument. The high flux neutrons and easy access open sample space make the instrument capable of tackling a wide variety of engineering and materials science experiments under extreme conditions, including deformation mechanisms of structural and functional materials, phase transformation and transition kinetics of energy materials, residual stress and phase mapping in engineering structures and texture etc., from fundamental to applied researches.

1. Instrument characteristics

As shown in Fig. 4(a) and the specification Table V, the current detector coverage on VULCAN, concentrated at 20-scattering angles of $\pm 90^\circ$, represents about one third of the fully built out detector solid angle proposed for the instrument. The incident beam spectra can be freely chosen during an experiment from different bandwidths/centers provided by

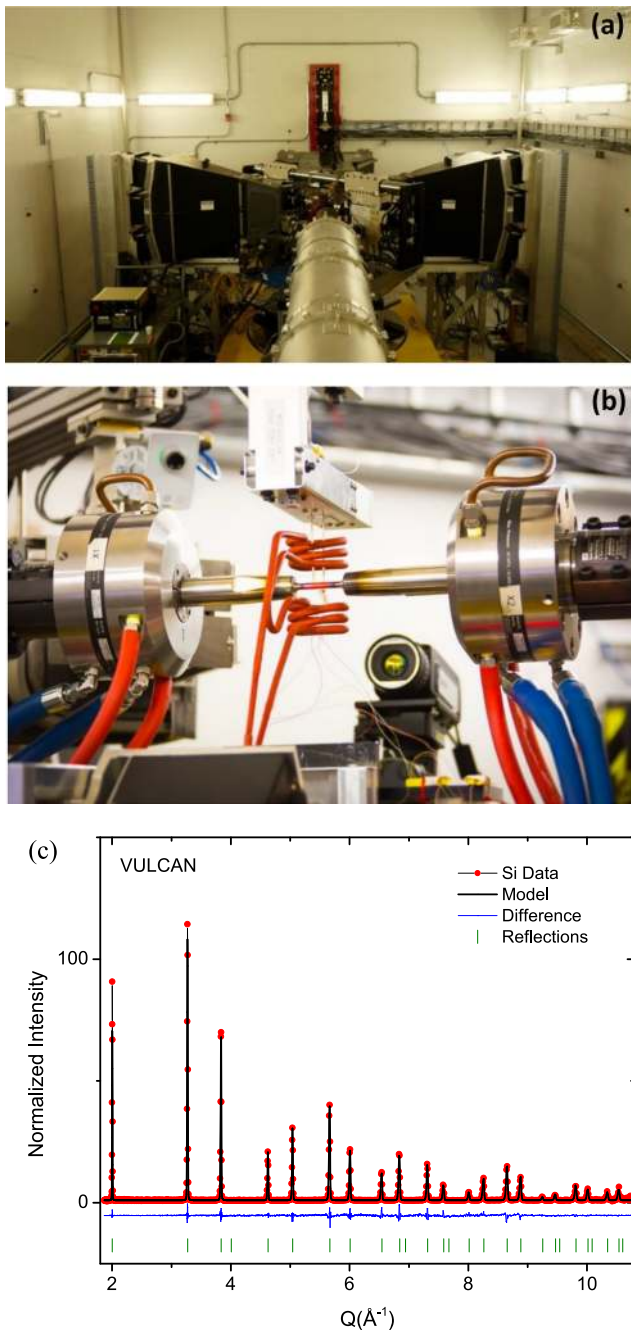


FIG. 4. (a) VULCAN instrument with the VULCAN-MTS load frame on the sample stage. (b) A typical *in situ* thermomechanical diffraction experimental setup on VULCAN, the tensile metallic sample loaded in the VULCAN-MTS load frame, and heated in air by induction coils with a close loop control by the control thermocouple welded on the sample, the high temperature extensometer with alumina extension rods measures the macroscopic strain, and the infrared camera records the temperature distribution. (c) Si measurement at 20 Hz in high resolution mode. The data are normalized using vanadium, and the refinement was carried out using GSAS.

the double disk choppers. The typical measurement range in d-spacing is from 0.5 to 3.5 \AA (with 20 Hz chopper, 2.8 \AA central, and 4.32 \AA bandwidth incident wavelengths) with the 90° banks. The motorized incident slits provide a flexible beam opening range from 0.1 to 12 mm in both horizontal and vertical directions. Two sets of radial collimators of 2 mm and 5 mm are available for different receiving collimations. From the combination of the incident slits and collimators, VULCAN provides rapid volumetric mapping with a gauge volume of 2-600 mm^3 and measurement times of a few minutes for typical engineering materials. For example, for *in situ* deformation measurement of 6 mm diameter tension bars by ferric alloys, data are collected continuously and can be chopped into 1 min or less for lattice strain evolutions. Similar instruments at other neutron facilities include EnginX at ISIS, UK and Takumi at J-PARC, Japan.

Much of the scientific impact of VULCAN is due to dedicated sample environment equipment including a load frame capable of delivering multi-axial loadings (10 T axial, 400 Nm torsional) and fatigue tests (rated up to 30 Hz) with an induction heater up to 1273 K, see Fig. 4(b), high-temperature and controlled-atmosphere furnaces, and cells to study battery cycling. Other SNS sample environments with variable temperature and electric and magnetic fields can be adapted easily to VULCAN. The open access platform allows users to bring in lab-scale equipment for *in situ* materials studies. Time-resolved studies are routinely conducted thanks to both the friendly time event neutron DAQ and the corresponding data reduction software.^{43,44}

2. Science examples

Science examples on VULCAN include deformation mechanisms and texture of conventional engineering alloys widely used in industries,⁴⁵⁻⁴⁸ design of high entropy alloys⁴⁹⁻⁵¹ and superalloys,^{52,53} stress or temperature induced phase transformation of shape memory alloys^{54,55} and composites,^{56,57} synthesis or stability of energy materials such as energy storage materials,^{58,59} and energy conversion materials,⁶⁰ including battery materials performance under operando,^{61,62} *in situ* materials processing,⁶³ residual stress of additive manufactured structures,^{64,65} and load sharing in suspension bridge cable.⁶⁶ Stroboscopic approaches^{44,67} can be easily realized for rapid time resolved measurements.⁶⁸ Single crystal material behavior can also be studied under external fields by utilizing the 2D detector coverage.⁶⁹⁻⁷¹

E. HB-2A

The HB-2A powder diffractometer is primarily utilized for magnetic structure determination, with an emphasis on ultra-low temperatures combined with high field or pressure. The constant wavelength neutron beam, flat background, simple beam profile, and open instrument layout make HB-2A well-suited to a variety of interchangeable sample environments with minimal instrument calibration.

1. Instrument characteristics

HB-2A offers a balance of good Q-resolution while still maintaining much of the high intensity flux from the HB-2

TABLE V. BL-7 VULCAN instrument specifications.

Applications	Neutron beam	Resolution ($\Delta d/d$)	Q-range	Beam size at sample	Measurement times
Versatile materials engineering diffraction capabilities	TOF (poisoned decoupled ambient water)	High resolution mode: 2.5×10^{-3} high intensity mode: 4.5×10^{-3}	1.6-16 \AA^{-1} (at $2\theta = 90^\circ$)	V: 0.1–12 mm H: 0.1–12 mm	Seconds to minutes. Data collected continuously and binned based on required statistics

beam port at HFIR.⁷² This is achieved by using a vertically focused germanium monochromator with a fixed 90° take-off angle that selects the principle wavelengths of 2.41 \AA (Ge 113) and 1.54 \AA (Ge 115), see Table VI for the corresponding Q range covered. During experiments, the long wavelength is typically utilized for magnetic studies to access low Q with the highest resolution and lowest background, whereas the shorter wavelength affords larger coverage of reciprocal space for more detailed crystal structure refinements. Switchable pre-sample 16', 21', 31', and post sample fixed 12' Soller collimators offer further control of flux and resolution. The layout of HB-2A follows a Debye-Scherrer geometry with a detector bank consisting of 44 discrete ^3He detectors. The full detector coverage is $\sim 150^\circ$; however, the detector bank must be scanned to fill in the $\sim 2.6^\circ$ 2θ gaps between the detectors. The 44 pre-detector collimator replacement from 6' to 12' was the most recent upgrade since the instrument entered the user program in 2009. This improved the detected intensity by more than a factor of 2.5 and improved the signal-to-noise ratio by 1.5 times. The HB-2A instrument design and operation is most similar to BT-1 at NIST and D2B at the ILL that are also composed of a detector bank of separated ^3He detectors.

Typical sample masses of 5 g and above make optimum use of the large beam size of $60 \times 20 \text{ mm}^2$ at sample; however, measurements on smaller samples are routinely performed with longer counting times. Refinable data for crystal structure modeling are readily achieved in under an hour. The counting times for magnetic signals scale with the ordered moment size and mass and therefore vary significantly between samples. Time scales for magnetic measurements range from under an hour up to 12 h on small samples with weak or diffuse magnetic signals. Additionally, setting up complex sample environments, such as dilution refrigerators, can take several hours; therefore, suitable experimental planning with beamline staff is required to appropriately allocate time.

To further complement magnetic studies, HB-2A has implemented a polarized incident neutron beam option before the sample that offers extreme sensitivity to small magnetic

signals, under $0.1 \mu_B$, in materials with ferromagnetic or ferromagnetic components to the moment,⁷³ see Fig. 5(a). Both He-3 filter and supermirror options have been used, with the supermirror V-cavity the standard option offered to users.

The open instrument layout offers the option to host and easily switch between a variety of sample environments with minimal instrument calibration. Ultra-low temperature measurements in dilution (50 mK) and He³ (280 mK) inserts, applied magnetic fields (6 T), and pressure cells (2 GPa) are routinely performed along with traditional cryostats (1.5 K) and air or vacuum furnaces (up to 1800 K). Room temperature measurements on multiple samples can be performed with a 6-carousel sample changer. A 3-sample stick has recently been implemented into the orange cryostat (1.5-300 K), with similar capabilities for other sample environments under development.

2. Science examples

The core of the science performed on HB-2A is focused on the investigation of magnetic structures in crystalline materials as a function of temperature, field, and pressure. Detailed analysis of complex magnetic structures often requires representational analysis or magnetic symmetry techniques, see Sec. III B.

Science examples on HB-2A include studies of materials with strong spin-orbit interactions that show coupling between magnetism and lattice or electronic conduction,^{74–76} magnetic order in multiferroic materials,^{77–79} geometrically frustrated magnetism at ultra-low temperatures,⁸⁰ thermoelectric materials,⁸¹ low-dimensional magnetism,^{82,83} quantum critical phenomena,⁸⁴ and pressure controlled materials. The implementation of half-polarization has been demonstrated and is a potential growth area for new science at the instrument.⁷³

F. WAND²

The HFIR WAND² instrument is a high intensity dual-purpose powder/single-crystal diffractometer, supported by the US–Japan Cooperative Program on Neutron Scattering.

TABLE VI. HB-2A POWDER instrument specifications.

Applications	Neutron beam	Resolution ($\Delta d/d$)	Q-range	Beam size at sample	Measurement times
Magnetic structure determination under extreme environments. Polarized beam option	Constant wavelength (vertically focused Ge monochromator)	2.2×10^{-3} (variable)	0.2-5.1 \AA^{-1} ($\lambda = 2.41 \text{\AA}$) 0.35-8 \AA^{-1} ($\lambda = 1.54 \text{\AA}$)	$60 \times 30 \text{ mm}$ Typical can sizes are 6-15 mm diameter and 50 mm height	Variable. Refinable data in minutes. Magnetic structure in 0.5–8 h

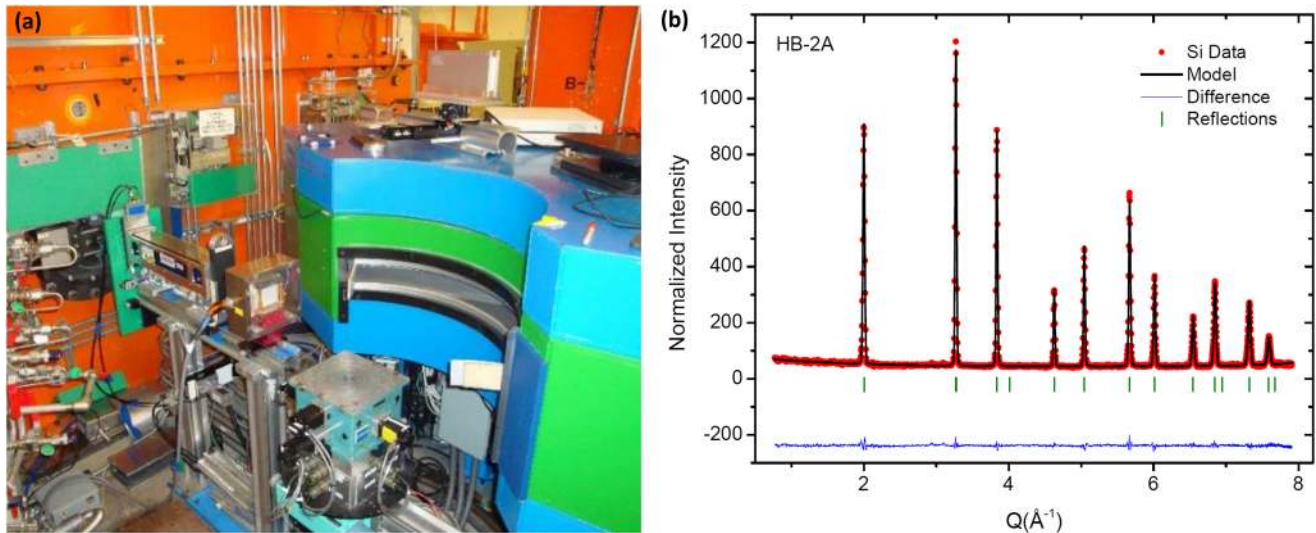


FIG. 5. (a) Incident neutron beam polarization set-up with supermirror V-cavity and flippers. The open goniometer sample area is shown. (b) Si data collected on HB-2A using a wavelength of 1.54 Å. Measurements were collected at room temperature with the sample loaded into a vanadium holder in the six-sample changer. Detector efficiency is normalized with vanadium. Rietveld refinement was performed using Fullprof.

1. Instrument characteristics

WAND² has just completed its second and final upgrade phase, which amounts to a complete replacement of the whole instrument after the monochromator (Table VII). The instrument now supports a diverse array of sample environments, including ultralow temperature (50 mK), high pressure (up to 5 GPa), and high magnetic field (6 T) (Fig. 6). A major part of the upgrade was the deployment of a large 2D position sensitive detector with nearly 2×10^6 pixels which expands the instrument beyond simply mapping reciprocal space to providing quantitative 3D intensities.⁸⁵

WAND² has a low monochromator take-off angle, which reduces the Q -resolution, but allows for high intensity to access high data rates and small samples. Powder diffraction studies using WAND² necessarily involve materials that have simple crystal structures and/or small unit cell volumes. However, it can and has been used for kinetic studies where structural changes can be seen to evolve on a time scale of a few minutes. The data rate achievable from the new detector will enable kinetic studies over time scales of seconds.

The exceptionally high flux on WAND² allows experiments to undertake *in situ* studies, follow chemical reactions and other kinetic processes. Furthermore, WAND² takes data in event mode which opens the possibility to filtering data after the experiment or synchronizes the data stream to an external input for stroboscopic measurements.

In this respect, WAND² will compete with already mature and successful 2D PSD instruments with comparable flux at ANSTO (WOMBAT) and ILL (D19 and D20). Compared to these instruments, WAND² has less flexibility in varying intensity and resolution settings due to only one fixed monochromator position. A planned next upgrade for WAND² foresees the installation of an additional monochromator position to allow a high flux option with a pyrolytic graphite monochromator and a high-resolution option using the existing germanium monochromator, an option the other diffractometers already have. The identical detectors of WOMBAT and WAND² are gapless with higher intrinsic resolution, which can be important in the studies of texture. They also operate at higher ³He pressures which should translate into higher efficiency. Time resolution for stroboscopic measurements on WAND² can be achieved down to 100 ns (10 MHz), two orders of magnitude better than the other instruments. Data acquisition on WAND² is continuous, allowing *a posteriori* time slicing.

The space in the incident beam path also allows for a polarization device, either He-3 filter or supermirror, and this option can be a beneficial addition for magnetic structural studies of ferro- or ferrimagnetic components in both powder and single-crystal modes of operation for WAND². Overall, these recent upgrades have made this instrument a state-of-the-art tool in the powder diffraction suite on the North American continent.

TABLE VII. HB-2C WAND² instrument specifications.

Applications	Neutron beam	Resolution ($\Delta d/d$)	Q -range	Beam size at sample	Measurement times
General purpose diffraction/diffuse scattering under extreme sample environments	Constant wavelength (vertically focused Ge monochromator)	2×10^{-2}	$0.1\text{-}8.2 \text{\AA}^{-1}$	$30 \times 40 \text{ mm}^2$ (full size) $9.6 \times 40 \text{ mm}^2$ (motorized slits)	5 min for high statistics. Refinable data in 1 s

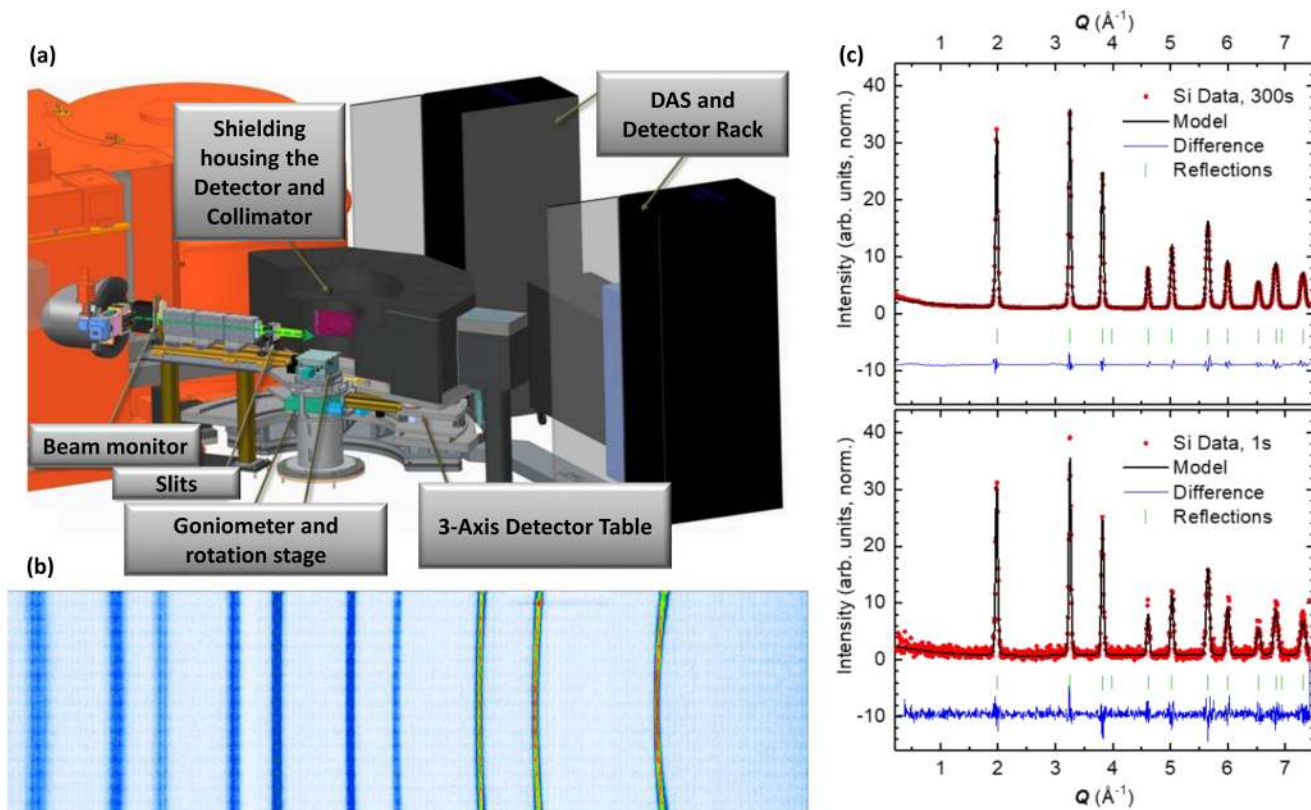


FIG. 6. (a) Schematic of the WAND² instrument sample area with the main components. (b) Detector view of the powder diffraction pattern from a Si-Standard sample using a wavelength of 1.487 Å (2θ from right to left). (c) Reduced WAND² measurements of Si standard for two data acquisition times (300 s, top; 1 s bottom). Refinement was performed with Fullprof.

2. Science examples

WAND² was commissioned in February 2018 and returned to the user program in May 2018. Therefore, no data has been published so far using the new detector. From the first user experiments, it is expected that magnetic structural studies will make up a major part of WAND²'s scientific portfolio; however, the instrument's versatility also enables studies in other areas such as lipid bilayer diffraction⁸⁶ and oxygen diffusion in Ruddlesden-Popper phases.⁸⁷

III. NEUTRON POWDER DIFFRACTION SUITE CAPABILITIES

A. Sample environment capabilities and development across the suite

The powder diffraction suite can access an extremely large parameter space of temperature, magnetic and electric field, pressure, and atmosphere. A suite-wide guide of common sample environments is summarized in Table VIII. These capabilities are essential at the forefront of neutron scattering science, where powder diffraction is generally the first choice for explorative investigations due to the accessible data, mature analysis software, and less demanding sample synthesis requirements.

The HB-2A and WAND² at HFIR offer a wide variety of sample environments, with all capabilities available on both instruments due to the identical sample goniometers.

The dilution refrigerator (DR) and He³ inserts available can additionally be combined with the cryo-magnets to achieve a parameter space down to 50 mK and up to 5 T in a single measurement. A new workhorse 6 T magnet is being purchased for HFIR to complement the magnetic studies at HB-2A and WAND². Development of clamp style pressure cells through the US-Japan program that can be easily cooled to 4 K has been successfully deployed on both instruments. Testing of the palm cubic anvil cell (up to 10 GPa) on WAND² is underway. High pressure combined with low temperature and magnetic field can further expand the experimentally accessible phase space.

The SNAP diffractometer has been a pioneer in developing diamond anvil cell (DAC) technology for neutron diffraction and an initial type of a neutron DAC achieved a record 90 GPa pressure in collaboration with the Geophysical Laboratory. Throughout the last 3 years entirely new cells based on ultra-large synthetic diamonds have been developed in-house. These cells, which allow for the first time the study of a range of materials with more complex crystalline or even disordered structures and can be cooled to 5 K, have now become available in the user program.

For the study of liquids and glasses under extremely high temperature, the NOMAD team and outside collaborators have developed neutron-friendly aerodynamic and electrostatic levitators. The standard sample environment capability for both POWGEN and NOMAD includes 2-300 K orange cryostat, 1200 C ILL furnace, and sample-changer fitted with CCR: 10-300 K (POWGEN) and Cryostream: 100-500 K

TABLE VIII. ORNL powder suite sample environment capabilities.

	BL-1B NOMAD	BL-11A POWGEN	BL-3 SNAP	BL-7 VULCAN	HB-2A POWDER	HB-2C WAND ²
Temperature (K)	Sample-changer: 90-500. Orange cryostat: 2-300. ILL furnace: 300-1500. Levitator: 800-3000.	24 sample-changer: 12-300 Orange cryostat: 2-300 ILL furnace: 300-1500	2-350 clamp cell 10-350 DAC 85-350 PE cell 300-1500 PE cell furnace	Load frame with cooling to 190 and heating up to 1273. Orange cryostat: 2-300. ILL furnace: 300-1873.	DR insert: 0.05-300. He ³ insert: 0.3-300. Orange cryostat: 1.5-300 (3-sample changer). Top loading: CCR: 4-700. Vacuum/air furnace: 300-1800.	DR insert: 0.05-300. He ³ insert: 0.3-300. Orange cryostat: 1.5-300 (3-sample changer). Top loading: CCR: 4-700. Vacuum/air furnace: 300-1800.
Pressure (GPa)	Gas cell: 0.2	Pressure capabilities are under development	DAC: 40 PE cell: 20 PE cell: 6 clamp cell: 2 gas cell: 0.6	Uniaxial, multiaxial loading fatigue load frame with 10 T force and 400 Nm torque	Clamp cell: 2 Gas cell: 0.6	<0.6 gas cell <2 clamp cell
Magnetic field (T)	Not fully commissioned	<5	Not currently available	<5	<6	<6
Additional sample environments	Electric field: ± 10 kV Gas handling with pO ₂ and RGA	Gas handling with pO ₂ and RGA	Electric field: ± 10 kV. Gas handling with pO ₂ and RGA, resistive heating gas enclosure load frame (RHEGAL), mini load frame, large sample/structure heating by induction, sample texture rotation stages, friction stirring welder/processor	6-sample changer (room temperature). Electric field: ± 5 kV	6-sample changer (room temperature). Humidity chamber. Electric field: ± 5 kV	

(NOMAD). Gas-handling capability is available on POWGEN, with future development aimed at supplying more turnkey gas-handling system, atmosphere furnace, gas pressure cells, and gas absorption setups to serve a growing user community.

VULCAN focuses on materials design, processing, and performance, and the major sample environment development efforts are for realizing practical materials behavior under external stimuli. In addition to the VULCAN-MTS load frame, special sample environments such as resistive heating gas enclosure load frame⁶⁷ and neutron friction stirring welder/processor⁶³ are developed for materials physical behavior simulations. A compact paper size mini-load frame is available for VULCAN as well as for use at other suites.⁸⁸

B. Structural studies and computational tools

One of the primary reasons for the success of powder instruments can be assigned to the impressive community development of standard analysis codes, including GSAS (with GSAS-II including TOF data analysis),⁸⁹ Fullprof,⁹⁰ JANA,⁹¹ RIETAN,⁹² MAUD,⁹³ PDFGetN,⁹⁴ PDFfit⁹⁵ and RMC-profile.⁹⁶ There is a consistent expectation across the powder suite to provide users with data both fully calibrated and normalized against, for instance, incident spectra and detector efficiency. In addition, more advanced analysis routines are being implemented for unique cases, for example, at SNAP, the necessary corrections for measurements through large strained diamonds⁹⁷ are currently being implemented into ORNL software.

Magnetic structure determination is best accomplished using neutron diffraction. Measurements generally require collecting data at low temperature in the magnetically ordered phase and at a higher temperature, above the transition, in the paramagnetic regime. More advanced studies incorporate applied magnetic fields and high pressure. Polarization analysis is available on HB-2A and WAND² as a further and highly sensitive step to discriminate the magnetic signal. In a separate direction recently, magnetic studies have expanded into the total scattering regime with magnetic PDF measurements (mPDF).^{98,99} In general, magnetic structural studies continue to become ever more complex, covering ordering

including modulated structures, large cells, reduced dimensionalities manifesting diffuse scattering and geometrically frustrated systems that do not order without perturbations. Data analysis is therefore increasingly more important as complexity grows, with representational analysis and magnetic symmetry techniques often required. Typically utilized software for dedicated magnetic structure determination includes Sarah,¹⁰⁰ BasiRep,⁹⁰ Isodistort,¹⁰¹ JANA,⁹¹ and the Bilbao Crystallographic server.¹⁰²

In advanced computation, there are efforts throughout ORNL to utilize powder diffraction measurements for advanced analysis. While the standard refinement methods and tools offer deep insights, expanding beyond these capabilities is often required for new scientific discoveries. For example, the resulting time averaged structure measured with powder diffraction and responses to perturbations are intimately linked with deeper underlying physical phenomena, such as superconductivity, charge transfer, and exotic magnetism, which cannot be fully elucidated by a set of refinements alone. Instead the data must be coupled with sophisticated computational tools. To this effect, there are several opportunities to harness the computational power available at ORNL to test hypothesis and validate computational models of complex systems with powder data. Examples include the determination of diffusion paths and energy barriers estimation in ionic conductions or battery materials, the interpretation of nuclear and magnetic diffuse scattering to access disorder, and the understanding of the underlying nature of phase transitions via the analysis of critical exponents of order parameters. This coupling between high performance computing and machine learning will be a major growth area and go hand in hand with future diffractometer capabilities and developments.

C. Total scattering analysis

Both NOMAD and POWGEN TOF powder diffractometers access the needed Q range and resolution for neutron total scattering studies with pair distribution function (PDF) data. The newly updated detector configuration at POWGEN allows suitable data to be collected in a single frame, providing recently expanded opportunities for local structure studies in the suite. Figure 7 shows a comparison of typical NOMAD and

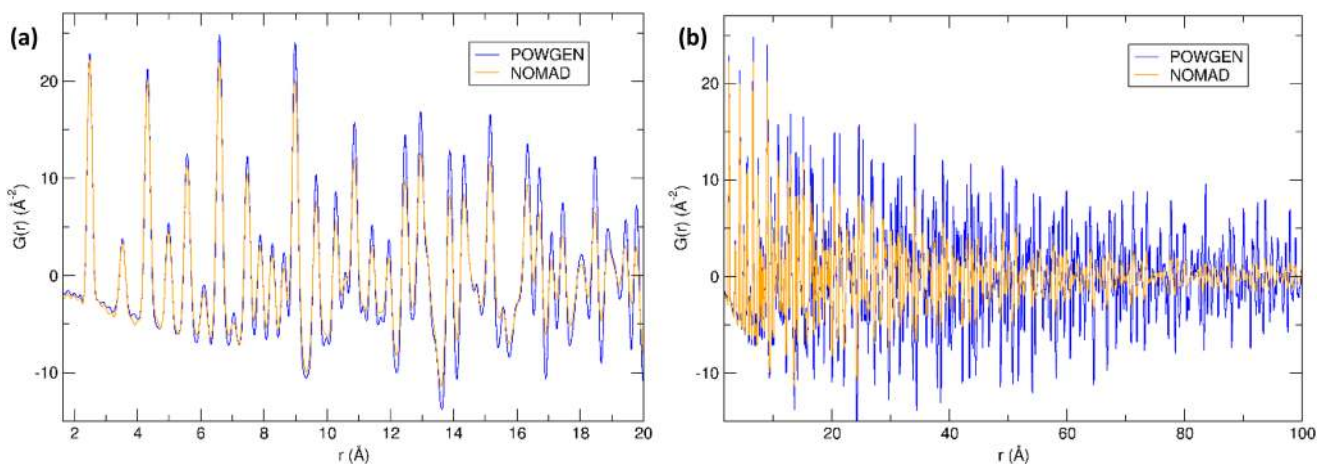


FIG. 7. (a) Low- r and (b) high- r comparison of Ni PDF data available at the POWGEN instrument (in blue) and the NOMAD instrument (in orange).

POWGEN PDF data collected for Ni powder. For NOMAD, the data were measured in a 6 mm vanadium canister for 30 min, while for POWGEN the data were measured in an 8 mm vanadium canister for 3 h. The instruments produce similar low- r data, with the primary difference between datasets being the higher dampening envelope in the NOMAD case, an effect of both its lower resolution and more asymmetric peak shapes.

NOMAD is the dedicated total scattering beamline in the powder diffraction suite, and due to its high intensity and initial design focus, it is the best choice for local structure studies of amorphous, liquid, and nanocrystalline materials, and for the study of time-resolved phenomena or small samples involving disordered crystalline materials. On the other hand, POWGEN provides superior real space data in the intermediate to high- r (20 Å and up) range, making it an attractive capability for disordered crystalline material studies focusing on this intermediate length scale range, as well as a convenient add-on option when pursuing detailed average structure studies at the instrument. The newly updated detector configuration at POWGEN has made PDF studies feasible in the 3–8 h standard measurement times per data point at the instrument. Increased utilization of this capability is thus anticipated. However, it should be stressed that these are representative times of typical measurements rather than best possible measurements at the instruments. The respective data characteristics and options with regards to PDF studies in the suite will be explored in detail in a future contribution.

IV. FUTURE NEUTRON POWDER DIFFRACTION INSTRUMENTATION

A. Upgrades to current instruments in the powder suite

NOMAD: A clear route to increase the count rate is to fill out the detector bank complement that currently only has a 50% population of the available detector positions. Full detector coverage coupled with SNS running at the design power of 1.4 MW will bring NOMAD's c-number (=neutrons scattered from 1 cm³ Vanadium per second and 0.05 Å⁻¹ bandwidth) to about a factor of 4 higher. This world-leading neutron flux will realize a long-term vision toward areas that increasingly take advantage of very fast data rates and wide angular coverage, characterizing atomic structure in an increasing array of *in situ* and *in operando* phenomena (see Olds *et al.* in this issue), and facilitating new community growth areas such as multi-length scale structural, direction (orientation) dependent local structure (see Usher *et al.* in this issue), and diffuse magnetic structure studies.^{98,99} It is also clear that NOMAD will continue to have a central and sustainable role in the study of liquid, glass, and other amorphous material studies, especially as an increasing number of research groups are turning to nature for inspiration, exploiting non-equilibrium, metastable amorphous, and disordered materials motifs to attain materials with novel and more tunable properties.

POWGEN: The first stages of planned upgrades to POWGEN were completed in early 2018 with the installation of half the anticipated detector coverage. New detectors based on similar wavelength shifting fiber technology are now

being developed to improve the spatial resolution for the next generation detectors. These detectors are needed for the out of plane location, especially in backscattering and forward scattering angles, to maintain the resolution needed for the third-generation design of the POWGEN.

SNAP: To further improve the capabilities of SNAP for extremely small samples, and thus increase available pressures, SNAP is currently undergoing several upgrades. First, the upgrade of its detectors has now been completed and is currently being commissioned. This upgrade addressed the wear and tear of a decade of operation and will result in an upgraded version of the optical package. In addition, the new detectors exhibit improved special homogeneity and increased gamma ray discrimination, a known issue in this type of detector especially when located in such a short, high flux, beamline. Commissioning of the new detectors indicated significant improvement in signal-to-background ratio of 3.5 times. This is expected to improve further once the full upgrade is deployed. In addition, there is an ongoing project that aims at replacing the existing focusing optics with ones with improved geometry that are better matched to the new standard sample sizes. These upgrades will further improve data quality, enable the expansion of the pressure capabilities, as well as shorten necessary exposure times.

VULCAN: An upgrade project to build out the VULCAN detectors, at 120°, 150°, -60°, and -150°, has been initiated and the plan with high spatial resolution ³He detectors (5 × 6 mm² pixilation) will provide significant gains in both efficiency, factor ×2, and resolution per unit area, factor ×17. The expanded detector angular coverage and efficiency gains, coupled with high spatial resolution, will increase capabilities by an order of magnitude for measurements of real-time operations whilst offering new capabilities in areas such as high-spatial resolution mapping in residual stress, grain orientations, and interfacial lattice strain deformation,¹⁰³ probing the evolution of dislocation densities under extreme conditions and *in situ* measurement of pole figures under load.

HB-2A: The current detector design of a bank of 44 spaced He³ tube detectors requires scanning of the detector bank to fill in the ~3° angular gaps and achieve a standard diffraction pattern. Replacement with a position sensitive detector, that is now commonly found on reactor-based diffraction instruments such as D20 at ILL, WOMBAT at ANSTO, or HRPT at PSI, would increase the count rate by a factor of ×50. This dramatic increase would allow HB-2A to become a world class diffractometer. New capabilities would include the ability to measure mg sized samples, achieve detailed parametric studies of temperature, pressure, field, voltage that is currently unfeasible and undertake *in situ* time-resolved measurements.

WAND²: As part of the scheduled Be-change out at HFIR in 2022, a modification of the HB-2 beam tunnel is planned. This would incorporate two monochromator positions for WAND². One would be close to the current layout at small take-off angles (~41°) for a high-flux, low resolution option using for instance a fixed focused pyrolytic graphite monochromator. Further downstream, an additional monochromator position could house the current Ge-monochromator at a higher take-off angle (~100°) for a low-flux, high resolution option.

B. New powder diffraction instruments at ORNL

Considering the powder suite collectively and, in particular, the two general purpose diffractometers at the SNS, NOMAD, and POWGEN, the user community has identified two priority areas for future instrument additions to the powder suite.

First, while POWGEN and NOMAD are highly complementary by being at either end of the flux-versus-resolution trade-off, to meet the needs of the materials development and powder diffraction communities, an instrument sited in the middle of these two extremes is required, such as the GEM and Polaris diffractometers at the ISIS neutron spallation source in the United Kingdom, the NOVA diffractometer at J-PARC in Japan, or the recently closed Neutron Powder Diffractometer (NPDF) instrument at Los Alamos National Laboratory's Lujan Center, leaving the United States without an instrument in this class. To this end a new instrument, DISCOVER, is being designed to fill this gap. DISCOVER is the evolution of the previous "RAPID" instrument concept, originally proposed at the June 2013 ORNL user workshop "Delivering on the Promise of Powder Diffraction." The change in name reflects its strategic place in the SNS diffraction suite: it will fill a current US capability gap between the high-flux wide-Q diffraction/total scattering instrument NOMAD and the medium-to-high-resolution powder diffraction instrument POWGEN. As such, DISCOVER will combine the characteristics of two enormously successful instruments: (1) the recently closed NPDF at Los Alamos National Laboratory, which was a world-class PDF diffractometer, despite being located on a relatively low-flux source and (2) the equally transformational characteristics of the Rapid acquisition PDF (RaPDF) development in the x-ray domain, leading to the highly successful 11-ID-B beamline at the Advanced Photon Source and XPD beamline at NSLS-II.

Second, the other priority to complete the general-purpose powder diffractometers at the SNS is an ultra-high-resolution instrument. ORNL currently hosts the highest resolution powder diffractometer in North America in POWGEN; however, the third-generation design was not intended for ultra-high-resolution studies that would aim to achieve 10^{-4} resolution over a wide d-spacing range. An instrument concept, HighResPD, is currently being developed to meet this need. Future opportunities at the FTS along with the planned second target station (STS) at ORNL are also under consideration to further expand the capabilities of the powder diffraction suite.

V. CONCLUSIONS

The suite of neutron powder diffractometers at ORNL allows researchers to study the crystal and magnetic structures of almost any powder material over a wide range of reciprocal and parameter phase space using traditional Rietveld refinement or PDF quality data. Future instrument upgrades and proposed new instruments will further enhance capabilities to create a world leading powder diffraction suite at ORNL.

ACKNOWLEDGMENTS

We thank the support staff at ORNL and the scientific associates who help ensure the instruments and experiments run as efficiently and effectively as possible. The research at ORNL's High Flux Isotope Reactor and Spallation Neutron Source was sponsored by the Scientific User Facilities Division, Office of Basic Energy Sciences, U.S. Department of Energy.

This manuscript has been authored by UT-Battelle, LLC under Contract No. DE-AC05-00OR22725 with the U.S. Department of Energy. The United States Government retains and the publisher, by accepting the article for publication, acknowledges that the United States Government retains a non-exclusive, paid-up, irrevocable, worldwide license to publish or reproduce the published form of this manuscript, or allow others to do so, for United States Government purposes. The Department of Energy will provide public access to these results of federally sponsored research in accordance with the DOE Public Access Plan (<http://energy.gov/downloads/doepublic-access-plan>).

- ¹J. Neufeind, M. Feyngenson, J. Carruth, R. Hoffmann, and K. K. Chiple, *Nucl. Instrum. Methods Phys. Res., Sect. B* **287**, 68–75 (2012).
- ²S. Ikeda and J. Carpenter, *Nucl. Instrum. Methods Phys. Res., Sect. A* **239**, 536 (1985).
- ³L. Santodonato, Y. Zhang, M. Feyngenson, C. M. Parish, M. C. Gao, R. Weber, J. Neufeind, Z. Tang, and P. Liaw, *Nat. Commun.* **6**, 5964 (2015).
- ⁴L. Skinner, C. Benmore, J. K. Weber, J. Du, J. Neufeind, S. Tumber, and J. Parise, *Phys. Rev. Lett.* **112**, 157801 (2014).
- ⁵H. Wang, M. Naguib, K. Page, D. Wesolowski, and Y. Gogotsi, *Chem. Mater.* **28**, 349 (2016).
- ⁶D. S. Charles, M. Feyngenson, K. Page, J. Neufeind, W. Xu, and X. Teng, *Nat. Commun.* **8**, 15520 (2017).
- ⁷S. Lan, X. Wei, J. Zhou, Z. Lu, X. Wu, M. Feyngenson, J. Neufeind, and X. Wang, *Appl. Phys. Lett.* **105**, 201906 (2014).
- ⁸H. Wang, D. Wesolowski, T. Proffen, L. Vlcek, W. Wang, L. Allard, A. Kolesnikov, M. Feyngenson, L. Anovitz, and R. Paul, *J. Am. Chem. Soc.* **135**, 6885 (2013).
- ⁹H. Wang, L. Daemen, M. Cheshire, M. Kidder, A. Stack, L. Allard, J. Neufeind, D. Olds, J. Liu, and K. Page, *Chem. Commun.* **53**, 20 (2017).
- ¹⁰T. C. Fitzgibbons, M. Guthrie, E. Xu, V. Crespi, S. Davidowski, G. Cody, N. Alem, and J. Badding, *Nat. Mater.* **14**, 43–47 (2015).
- ¹¹J. Shamblyn, M. Feyngenson, J. Neufeind, C. Tracy, F. Zhang, S. Finkeldei, D. Bosbach, H. Zhou, R. Ewing, and M. Lang, *Nat. Mater.* **15**, 507 (2016).
- ¹²J. Song, L. Wang, Y. Lu, J. Liu, B. Guo, P. Xiao, J. J. Lee, X. Yang, G. Henkelman, and J. Goodenough, *J. Am. Chem. Soc.* **137**, 2658 (2015).
- ¹³X. Rong, J. Liu, E. Hu, Y. Liu, Y. Wang, J. Wu, X. Yu, K. Page, Y. Hu, W. Yang, H. Li, X. Yang, L. Chen, and X. Huang, *Joule* **2**(1), 125–140 (2018).
- ¹⁴B. Cao, G. Veith, J. Neufeind, R. Adzic, and P. Khalifah, *J. Am. Chem. Soc.* **135**(51), 19186 (2013).
- ¹⁵D. Chen, J. Neufeind, K. Koczkur, D. Bish, and S. Skrabalak, *Chem. Mater.* **29**, 6525 (2017).
- ¹⁶J. Liu, D. Olds, R. Peng, L. Yu, G. Foo, S. Qian, J. Keum, B. Guiton, Z. Wu, and K. Page, *Chem. Mater.* **29**, 5591 (2017).
- ¹⁷B. Li, H. Wang, Y. Kawakita, Q. Zhang, M. Feyngenson, H. Yu, D. Wu, K. Ohara, T. Kikuchi, K. Shibata, T. Yamada, X. Ning, Y. Chen, J. He, D. Vahnin, R. Wu, K. Nakajima, and M. Kanatzidis, *Nat. Mater.* **17**, 226–230 (2018).
- ¹⁸P. Radaelli, "Extending the domain of time-of-flight powder diffraction techniques," in *The Fourteenth Meeting of the International Collaboration on Advanced Neutron Sources* (1998), Vol. 2, available at <http://www.neutronresearch.com/proc/?y=1998;n=1;o=0>.
- ¹⁹A. Huq, J. Hodges, O. Gourdon, and L. Heroux, *Z. Kristallogr.* **1**, 127–135 (2011).
- ²⁰E. Talaie, V. Duffort, H. Smith, B. Fultz, and L. Nazar, *Science* **8**, 2512–2523 (2015).

- ²¹V. Duffort, E. Talaie, R. Black, and L. F. Nazar, *Chem. Mater.* **27**(7), 2515–2524 (2015).
- ²²T. Thompson, A. Sharafi, A. Huq, J. L. Allen, J. Wolfenstine, and J. Sakamoto, *Adv. Energy Mater.* **5**(11), 1500096 (2015).
- ²³A. B. Munoz-Garcia, D. E. Bugaris, M. Pavone, J. P. Hodges, A. Huq, F. Chen, H. Z. Loye, and E. A. Carter, *J. Am. Chem. Soc.* **134**, 6826–6833 (2012).
- ²⁴M. A. Tamimi and S. McIntosh, *J. Mater. Chem. A* **2**, 6015–6026 (2014).
- ²⁵J. Ma, O. Delaire, A. F. May, C. E. Carlton, M. A. McGuire, L. H. VanBebber, D. L. Abernathy, G. Ehlers, T. Hong, A. Huq, W. Tian, V. M. Keppens, Y. Shao-Horn, and B. C. Sales, *Nat. Nanotechnol.* **8**, 445–451 (2013).
- ²⁶C. W. Li, J. Ma, H. B. Cao, A. F. May, D. L. Abernathy, G. Ehlers, C. Hoffmann, X. P. Wang, T. Hong, A. Huq, O. Gourdon, and O. Delaire, *Phys. Rev. B* **90**, 214303 (2014).
- ²⁷J. M. Allred, K. M. Taddei, D. E. Bugaris, M. Krogstad, S. Lapidus, D. Y. Chung, H. Claus, M. G. Kanatzidis, D. E. Brown, J. Kang, R. M. Fernandes, I. Eremin, S. Rosenkranz, O. Chmaissem, and R. Osborn, *Nat. Phys.* **12**, 493–498 (2016).
- ²⁸A. Banerjee, C. Bridges, J. Yan, A. Aczel, L. Li, M. Stone, G. Granroth, M. Lumsden, Y. Yiu, J. Knolle, S. Bhattacharjee, D. Kovrizhin, R. Moessner, D. Tennant, D. Mandrus, and S. Nagler, *Nat. Mater.* **15**, 733–740 (2016).
- ²⁹R. Boehler, J. Molaison, and B. Haberl, *Rev. Sci. Instrum.* **88**, 083905 (2017).
- ³⁰B. Haberl, S. Dissanayake, F. Ye, L. L. Daemen, Y. Cheng, C. W. Li, A.-J. (Timmy) Ramirez-Cuesta, M. Matsuda, J. J. Molaison, and R. Boehler, *High Pressure Res.* **37**, 495–506 (2017).
- ³¹M. Guthrie, R. Boehler, J. Molaison, B. Haberl, A. D. Santos, and C. Tulk, “Structure and disorder in ice VII on the approach to hydrogen-bond symmetrisation,” *Phys. Rev. B* (unpublished).
- ³²R. Boehler, M. Guthrie, J. Molaison, A. D. Santos, S. Sinogeikin, S. Machida, N. Pradhan, and C. Tulk, *High Pressure Res.* **33**(3), 546–554 (2013).
- ³³H. K. Mao *et al.*, *Science* **239**, 1131–1134 (1988).
- ³⁴P. Loubeyere, R. LeToullec, D. Hausermann, M. Hanfland, R. Hemley, H. Mao, and L. Finger, *Nature* **383**, 702–704 (1996).
- ³⁵S. Haravifard, A. Banerjee, J. Wezel, D. Silevitch, A. D. Santos, J. Lang, E. Kermarrec, G. Srajer, B. Gaulin, J. Molaison, H. Dabkowska, and T. Rosenbaum, *Proc. Natl. Acad. Sci. U. S. A.* **40**(111), 14372–14377 (2014).
- ³⁶J. Cheng, K. Kweon, S. Larregola, Y. Ding, Y. Shirako, L. G. Marshall, Z. Li, X. Li, A. D. Santos, M. Suchomel, K. Matsubayashi, Y. Uwatoko, G. Hwang, J. B. Goodenough, and J. Zhou, *Proc. Natl. Acad. Sci. U. S. A.* **112**(6), 1670–1674 (2015).
- ³⁷A. Schaeffer, W. Cai, E. Olejnik, J. J. Molaison, S. Sinogeikin, A. D. Santos, and S. Deemyad, *Nat. Commun.* **6**, 8030 (2015).
- ³⁸T. C. Fitzgibbons, “Synthesis of carbon materials via the cold compression of aromatic molecules and carbon nanostructures,” Ph.D. Dissertation, Pennsylvania State University (2014).
- ³⁹C. Tulk, S. Machida, D. Klug, H. Lu, M. Guthrie, and J. J. Molaison, *J. Chem. Phys.* **141**, 174503 (2014).
- ⁴⁰C. Tulk, D. D. Klug, A. M. D. Santos, G. Karotis, M. Guthrie, J. J. Molaison, and N. Pradhan, *J. Chem. Phys.* **136**, 54502 (2012).
- ⁴¹M. Guthrie, R. Boehler, C. A. Tulk, J. J. Molaison, A. M. D. Santos, K. Li, and R. J. Hemley, *Proc. Natl. Acad. Sci. U. S. A.* **110**(26), 10552–10556 (2013).
- ⁴²K. An, H. D. Skorpenske, A. D. Stoica, D. Ma, X. L. Wang, and E. Cakmak, *Metal. Mater. Trans. A* **42**, 95 (2011).
- ⁴³K. An, R. Riedel, S. Miller, J. Kohl, H. Choo, and J. Jones, “Asynchronous *in situ* neutron scattering measurement of 10 μ s transient phenomena at spallation neutron source,” Oak Ridge National Laboratory Report, Oak Ridge, 2012.
- ⁴⁴G. E. Granroth, K. An, H. L. Smith, P. Whitfield, J. C. Neuefeind, J. Lee, W. Zhou, V. N. Sedov, P. F. Peterson, and A. Parizzi, *J. Appl. Crystallogr.* **51**, 616 (2018).
- ⁴⁵W. Wu, K. An, L. Huang, S. Y. Lee, and P. K. Liaw, *Scr. Mater.* **69**, 358 (2013).
- ⁴⁶D. Yu, K. An, Y. Chen, and X. Chen, *Scr. Mater.* **89**, 45 (2014).
- ⁴⁷W. Wu, P. K. Liaw, and K. An, *Acta Mater.* **85**, 343 (2015).
- ⁴⁸G. M. Stoica, A. D. Stoica, K. An, D. Ma, S. C. Vogel, J. S. Carpenter, and X. L. Wang, *J. Appl. Crystallogr.* **47**, 2019 (2014).
- ⁴⁹Z. Y. Liu, S. Guo, X. J. Liu, J. C. Ye, Y. Yang, X. L. Wang, L. Yang, K. An, and C. T. Liu, *Scr. Mater.* **64**, 868 (2011).
- ⁵⁰E. W. Huang, D. J. Yu, J. W. Yeh, C. Lee, K. An, and S. Y. Tu, *Scr. Mater.* **101**, 32 (2015).
- ⁵¹H. L. Huang, Y. Wu, J. Y. He, H. Wang, X. J. Liu, K. An, W. Wu, and Z. P. Lu, *Adv. Mater.* **29**, 1701678 (2017).
- ⁵²D. Yu, H. Bei, Y. Chen, E. P. George, and K. An, *Scr. Mater.* **84–85**, 59 (2014).
- ⁵³S. Y. Huang, Y. F. Gao, K. An, L. L. Zheng, W. Wu, Z. K. Teng, and P. K. Liaw, *Acta Mater.* **83**, 137 (2015).
- ⁵⁴O. Benafan, R. D. Noebe, S. A. Padula II, D. J. Gaydos, B. A. Lerch, A. Garg, G. S. Bigelow, K. An, and R. Vaidyanathan, *Scr. Mater.* **68**, 571 (2013).
- ⁵⁵H. Yang, D. Yu, Y. Chen, J. Mu, Y. D. Wang, and K. An, *Mater. Sci. Eng.: A* **680**, 324 (2017).
- ⁵⁶G. Song, C. Lee, S. H. Hong, K. B. Kim, S. Y. Chen, D. Ma, K. An, and P. K. Liaw, *J. Alloys Compd.* **723**, 714 (2017).
- ⁵⁷D. M. Wang, Y. Chen, J. Mu, Z. W. Zhu, H. F. Zhang, Y. D. Wang, and K. An, *Scr. Mater.* **153**, 118 (2018).
- ⁵⁸L. Cai, Z. C. Liu, K. An, and C. D. Liang, *J. Mater. Chem. A* **1**, 6908 (2013).
- ⁵⁹Y. Chen, E. Rangasamy, C. R. D. Cruz, C. D. Liang, and K. An, *J. Mater. Chem. A* **3**, 22868 (2015).
- ⁶⁰F. Ren, R. Schmidt, J. K. Keum, B. S. Qian, E. D. Case, K. C. Littrell, and K. An, *Appl. Phys. Lett.* **109**, 081903 (2016).
- ⁶¹L. Cai, K. An, Z. L. Feng, C. D. Liang, and S. J. Harris, *J. Power Sources* **236**, 163 (2013).
- ⁶²H. D. Liu, Y. Chen, S. Hy, K. An, S. Venkatachalam, D. N. Qian, M. H. Zhang, and Y. S. Meng, *Adv. Energy Mater.* **6**, 1502143 (2016).
- ⁶³W. Woo, Z. Feng, X. L. Wang, D. W. Brown, B. Clausen, K. An, H. Choo, C. R. Hubbard, and S. A. David, *Sci. Technol. Weld. Joining* **12**, 298 (2007).
- ⁶⁴T. Watkins, H. Bilheux, K. An, A. Payzant, R. Dehoff, C. Duty, W. Peter, C. Blue, and C. Brice, *Adv. Mater.* **171**(3), 23 (2013).
- ⁶⁵K. An, L. Yuan, L. Dial, I. Spinelli, A. D. Stoica, and Y. Gao, *Mater. Des.* **135**, 122 (2017).
- ⁶⁶A. Brügger, S.-Y. Lee, J. Mills, R. Betti, and I. Noyan, *Exp. Mech.* **57**, 921 (2017).
- ⁶⁷K. An, D. P. Armitage, Z. Yu, R. W. Dickson, R. A. Mills, Z. Feng, and H. D. Skorpenske, “Rhegal: Resistive heating gas enclosure loadframe for in-situ neutron scattering,” *Rev. Sci. Instrum.* (in press).
- ⁶⁸Z. Z. Yu, Z. L. Feng, K. An, W. Zhang, E. D. Specht, J. Chen, X. L. Wang, and S. David, in *Trends in Welding Research: Proceedings of the 9th International Conference, Chicago, 2013*.
- ⁶⁹A. Pramanick, K. An, A. D. Stoica, and X. L. Wang, *Scr. Mater.* **65**, 540 (2011).
- ⁷⁰Y. Huang, K. An, Y. Gao, and A. Suzuki, *Metal. Mater. Trans. A* **49**, 740 (2018).
- ⁷¹J. Coakley, E. A. Lass, D. Ma, M. Frost, H. J. Stone, D. N. Seidman, and D. C. Dunand, *Acta Mater.* **136**, 118 (2017).
- ⁷²V. O. Garlea, B. C. Chakoumakos, S. A. Moore, G. B. Taylor, T. Chae, R. G. Maples, R. A. Riedel, G. W. Lynn, and D. L. Selby, *Appl. Phys. A* **99**(3), 531–535 (2010).
- ⁷³D. M. Pajeroski, V. O. Garlea, E. S. Knowles, M. J. Andrus, and M. F. Dumont, *Phys. Rev. B* **86**, 054431 (2012).
- ⁷⁴S. Calder, J. G. Vale, N. A. Bogdanov, X. Liu, C. Donnerer, M. Upton, D. Casa, A. Said, M. Lumsden, Z. Zhao, J. Q. Yan, D. Mandrus, S. Nishimoto, J. V. D. Brink, J. P. Hill, D. F. McMorrow, and A. D. Christianson, *Nat. Commun.* **7**, 11651 (2016).
- ⁷⁵Q. Cui, W. Fan, J.-G. Cheng, A. E. Taylor, S. Calder, M. McGuire, J.-Q. Yan, D. Meyers, X. Li, Y. Q. Cai, Y. Y. Jiao, Y. Choi, D. Haskel, H. Gotou, Y. Uwatoko, J. Chakhalian, A. D. Christianson, S. Yunoki, J. B. Goodenough, and J.-S. Zhou, *Phys. Rev. Lett.* **117**, 176603 (2016).
- ⁷⁶S. Calder, L. Li, Y. C. S. Okamoto, R. Mukherjee, D. Haskel, and D. Mandrus, *Phys. Rev. B* **92**, 180413(R) (2015).
- ⁷⁷L. Zhou, J. Dai, Y. Chai, H. Zhang, S. Dong, H. Cao, S. Calder, Y. Yin, X. Wang, X. Shen, Z. Liu, T. Saito, Y. Shimakawa, H. Hojo, Y. Ikuhara, M. Azuma, Z. Hu, Y. Sun, C. Jin, and Y. Long, *Adv. Mater.* **29**, 1703435 (2017).
- ⁷⁸X. Wang, Y. Chai, L. Zhou, H. Cao, C. D. Cruz, J. Yang, J. Dai, Y. Yin, Z. Yuan, S. Zhang, R. Yu, M. Azuma, Y. Shimakawa, H. Zhang, S. Dong, Y. Sun, C. Jin, and Y. Long, *Phys. Rev. Lett.* **115**, 087601 (2015).
- ⁷⁹T. Ferreira, G. Morrison, W. M. Chance, S. Calder, M. D. Smith, and H. C. Z. Loye, *Chem. Mater.* **29**(7), 2689–2693 (2017).
- ⁸⁰R. Rawl, L. Ge, H. Agrawal, Y. Kamiya, C. R. Dela Cruz, N. P. Butch, X. F. Sun, M. Lee, E. S. Choi, J. Oitmaa, C. D. Batista, M. Mourigal, H. D. Zhou, and J. Ma, *Phys. Rev. B* **95**, 060412(R) (2017).

- ⁸¹J. Mao, J. Shuai, S. X. Song, Y. Wu, R. Dally, J. Zhou, Z. Liu, J. Sun, Q. Zhang, C. D. Cruz, S. D. Wilson, Y. Pei, D. J. Singh, G. Chen, C. Chu, and Z. Ren, *Proc. Natl. Acad. Sci. U. S. A.* **114**(40), 10548–10553 (2017).
- ⁸²M. A. McGuire, J. Q. Yan, P. Lampen-Kelley, A. F. May, V. Cooper, L. Lindsay, A. Puretzky, L. Liang, S. KC, E. Cakmak, S. Calder, and B. C. Sales, *Phys. Rev. Mater.* **1**, 064001 (2017).
- ⁸³A. F. May, S. Calder, C. Cantoni, H. B. Cao, and M. A. McGuire, *Phys. Rev. B* **93**, 014411 (2016).
- ⁸⁴L. Poudel, A. May, M. Koehler, M. McGuire, S. Mukhopadhyay, S. Calder, R. Baumbach, R. Mukherjee, D. Sapkota, C. de la Cruz, D. J. Singh, D. Mandrus, and A. D. Christianson, *Phys. Rev. Lett.* **117**, 235701 (2016).
- ⁸⁵M. Frontzek, K. M. Andrews, A. B. Jones, B. C. Chakoumakos, and J. A. Fernandez-Baca, “The Wide Angle Neutron Diffractometer squared (WAND2) - Possibilities and future,” *Physica B: Condens. Matter* (in press).
- ⁸⁶D. Marquardt, M. Frontzek, Y. Zhao, B. C. Chakoumakos, and J. Katsaras, *J. Appl. Crystallogr.* **51**, 235–241 (2018).
- ⁸⁷M. Ceretti, O. Wahyudi, G. André, M. Meven, A. Villesuzanne, and W. Paulus, *Inorg. Chem.* **57**(8), 4657–4666 (2018).
- ⁸⁸D. J. Yu, K. An, C. Y. Gao, W. T. Heller, and X. Chen, *Rev. Sci. Instrum.* **84**, 105115 (2013).
- ⁸⁹A. Larson and R. V. Dreele, “General structure analysis system (GSAS),” Los Alamos National Laboratory Report LAUR 86-748, 1994.
- ⁹⁰J. Rodriguez-Carvajal, *Phys. B* **192**, 55 (1993).
- ⁹¹V. Petricek, M. Dusek, and L. Palatinus, *Z. Kristallogr. - Cryst. Mater.* **229**(5), 345–352 (2014).
- ⁹²F. Izumi and K. Momma, *Solid State Phenom.* **130**, 15–20 (2007).
- ⁹³M. Ferrari and L. Lutterotti, *J. Appl. Phys.* **76**(11), 7246–7255 (1994).
- ⁹⁴P. F. Peterson, M. Gutmann, T. Proffen, and S. J. L. Billinge, *J. Appl. Crystallogr.* **33**, 1192 (2000).
- ⁹⁵T. Proffen and S. J. L. Billinge, *J. Appl. Crystallogr.* **32**, 572 (1999).
- ⁹⁶M. G. Tucker, D. A. Keen, M. T. Dove, A. L. Goodwin, and Q. Hui, *J. Phys.: Condens. Matter* **19**, 335218 (2007).
- ⁹⁷M. Guthrie, C. Pruteanu, M. Donnelly, J. Molaison, A. d. Santos, J. Loveday, R. Boehler, and C. Tulk, *J. Appl. Crystallogr.* **50**, 76–86 (2017).
- ⁹⁸B. A. Frandsen, X. Yang, and S. Billinge, *Acta Crystallogr., Sect. A: Found. Adv.* **70**, 3–11 (2014).
- ⁹⁹B. A. Frandsen, M. Brunelli, K. Page, Y. J. Uemura, J. B. Staunton, and A. S. J. Billinge, *Phys. Rev. Lett.* **116**, 197204 (2016).
- ¹⁰⁰A. S. Wills, *Phys. B* **276**, 680–681 (2000).
- ¹⁰¹B. J. Campbell, H. T. Stokes, D. E. Tanner, and D. M. Hatch, *J. Appl. Crystallogr.* **39**, 607–614 (2006).
- ¹⁰²M. I. Aroyo, J. M. Perez-Mato, D. Orobengoa, E. Tasci, G. D. L. Flor, and A. Kirov, *Bulg. Chem. Commun.* **43**(2), 183–197 (2011).
- ¹⁰³W. Wu, A. D. Stoica, K. D. Berry, M. Frost, H. D. Skorpenske, and K. An, *Appl. Phys. Lett.* **112**(25), 253501 (2018).